minerals

MDPI

Article

Effect of Hydrogen Peroxide on the Thermal and Mechanical Properties of Lightweight Geopolymer Mortar Panels

Cleidson Alves [1], Fernando Pelisser [2,*], João Labrincha [3] and Rui Novais [3]

[1] Civil Engineering Department, Federal Institute of Santa Catarina—IFSC, Criciúma 88813-600, SC, Brazil
[2] Civil Engineering Department, Federal University of Santa Catarina—UFSC, Florianópolis 88040-900, SC, Brazil
[3] Department of Materials and Ceramic Engineering/CICECO, Campus Universitario de Santiago, University of Aveiro—UA, 3810-193 Aveiro, Portugal
* Correspondence: f.pelisser@ufsc.br; Tel.: +55-(48)-99116-3073

Abstract: Lightweight geopolymers have been researched and used in specific applications due to their differentiated properties and, particularly, due to the lower environmental impacts in their manufacture, mainly associated with the use of raw materials with a low environmental impact and the reduction in greenhouse gas emissions. In this study, light geopolymers, using metakaolin, sodium silicate, sodium hydroxide, and hydrogen peroxide (H_2O_2), were evaluated. The effects of H_2O_2 concentration were evaluated up to a concentration of 1% in pastes and mortars. The properties of thermal conductivity, density, compressive strength, and modulus of elasticity were determined. The simulation of the thermal transmittance of cladding panels applied to a facade was also performed. Mortars with a H_2O_2 concentration of 0.2% obtained a compressive strength of 18 MPa and thermal conductivity of 0.55 W/mK, which was 60% less than the thermal conductivity obtained for the reference composition. The simulation of a panel for use on a facade showed that the thermal resistance increased from 0.27 (m^2.K/W) to 0.42 (m^2.K/W), indicating the efficiency of the geopolymer for use as a thermal control material.

Keywords: lightweight geopolymer; eco-efficient; mortar

check for updates

Citation: Alves, C.; Pelisser, F.; Labrincha, J.; Novais, R. Effect of Hydrogen Peroxide on the Thermal and Mechanical Properties of Lightweight Geopolymer Mortar Panels. *Minerals* **2023**, *13*, 542. https://doi.org/10.3390/min13040542

Academic Editor: Alexander Mikhailovich Kalinkin

Received: 24 February 2023
Revised: 5 April 2023
Accepted: 7 April 2023
Published: 12 April 2023

Copyright: © 2023 by the authors. Licensee MDPI, Basel, Switzerland. This article is an open access article distributed under the terms and conditions of the Creative Commons Attribution (CC BY) license (https://creativecommons.org/licenses/by/4.0/).

1. Introduction

The growing demand for high-efficiency, low-cost, and low environmental impact, especially compared with conventional concrete produced with Portland cement, has promoted the development of clinker-free cementitious materials, including geopolymer cements (also called alkali-activated cements, AAC), acting to reduce the carbon footprint of construction projects [1,2]. Geopolymers result from amorphous to semicrystalline three-dimensional silicon-aluminate structures of the Poly(sialate), Poly(sialate-siloxo) and Poly(sialate-disiloxo) types [3].

The study of geopolymer cements is considered a challenging research area with the potential for great economic and environmental impacts. These cements can be produced using a wide variety of raw materials [1] since they do not require materials with a high degree of purity and uniformity, at competitive costs, with lower energy expenditure and low CO_2 emissions compared to Portland cement [2,4].

The efficiency of materials used in construction depends on their environmental characteristics, their function, and the desirable properties of the material for a given application. Currently, the thermal efficiency of buildings is valued for economic reasons, and above all due to environmental issues since thermal control in buildings is a fundamental performance requirement for users and is associated with energy consumption. To meet this objective, the thermal properties of materials, such as conductivity and the ability to absorb or reflect the sun's rays, are important for thermal performance and, consequently, energy expenditure in buildings.

Considering this effect, metakaolin-based geopolymers have the potential to meet these thermal insulation requirements due to two main effects: their higher thermal reflectance due to the whitish coloration provided by metakaolin, and their thermal insulation capacity when modified to porous geopolymer. Numerous articles have been published in recent years on porous geopolymers [5–10]. The most commonly used strategy to produce porous geopolymers involves mixing an air-incorporating agent, such as hydrogen peroxide, to the geopolymers paste. The typology and amount of foaming agent associated with the mixing design (e.g., the ratio of solid precursor to activator solution ratio) determines the final properties of the bodies produced. This procedure leads to the production of highly porous bodies showing thermal conductivities below 0.4 W/m.K [11], and often lower than 0.2 W/m.K [12] suggesting the viability of using these novel materials in thermal insulation applications as an alternative to the fossil fuel-derived foams such as expanded polystyrene and polyurethane. Despite the promising results regarding their thermal insulation ability, the mechanical properties of the geopolymer foams are generally poor (below 10 MPa) [8], restricting their use in other relevant applications as building materials such as cladding panels. For this application, the materials must combine thermal insulation with adequate compressive strength (20 MPa—ABNT NBR 15.498) [13], and this remains challenging when considering geopolymer foams as to date most literature studies report moderate to low compressive strengths.

There are two main strategies for the synthesis of lightweight geopolymers, using either pore-forming agents (usually H_2O_2) and low-density aggregates. In the first line, the synthesis of lightweight geopolymer pastes, derived from fly ash and metakaolin, generally uses hydrogen peroxide as a foaming agent [14]. The compressive strength of the foams was strongly affected by the content of the foaming agent and the molarity of the sodium hydroxide solution. However, the compressive strength of the foams was always less than 5 MPa regardless of the composition. In another study [8], the synthesis of geopolymer foams using hydrogen peroxide solution with presented low apparent density (370–742 kg/m^3), low thermal conductivity (0.11–0.17 W/(m.K), high porosity (66–83 vol %), and acceptable compressive strength (0.3–11.6 MPa). The geopolymer foams showed good pore structure with 3.5% H_2O_2 and 2.85% sodium dodecyl sulfate, varying the dry density from 142 kg/m^3 to 1021 kg/m^3 and the compressive strength between 3.2 MPa and 44.8 MPa [15].

On the second line, geopolymer panels envisioned for the structural and energy retrofit of buildings, composed of fly ash and using expanded glass as an aggregate, achieved a maximum compressive strength of ~10 MPa, with an apparent density of approximately 1100 kg/m^3, and their thermal conductivity was 0.35 W/(m.K) [16]. The use of expanded polystyrene (EPS) grains as light aggregate has been also reported by [17]. The EPS-containing composites showed compressive strengths ranging from 15.8 to 26.4 MPa when the EPS content was 45% and 15%, respectively. Despite the interesting mechanical performance of these specimens, their synthesis is complex, requiring heat treatment at 350 °C for 12 h for the depolymerization of EPS, raising sustainability issues; furthermore, the thermal conductivity of the samples was not evaluated, and when studying geopolymers composed of EPS spheres, they achieved a high strength of approximately 50 MPa, although the thermal conductivity of the material was not measured [18]. Considering their application as structural materials, there is the challenge of obtaining strength with better efficiency or thermal conductivity. Considering the above, this research intends to develop lightweight geopolymers combining suitable mechanical strength, low thermal conductivity, and enhanced thermal efficiency to enable their use as cladding panels on building facades.

For this, geopolymeric pastes and mortars were produced with hydrogen peroxide as a pore-forming agent to be evaluated for their mechanical, physical, and thermal properties.

2. Materials and Methods

2.1. Materials

The following materials were used to produce the geopolymers: (i) kaolin of commercial origin from a company in southern Brazil (Esmalglass SA) was calcined in a laboratory oven at 800 °C for 3 h according to Rashad 2013 [19]; (ii) sodium silicate commercial origin from a company in southern Brazil (MQB of Brasil) (8.5% Na_2O, 29% SiO_2, 62.5% H_2O, by weight); (iii) sodium hydroxide NEON Commercial (97% pure NaOH); (iv) hydrogen peroxide Êxodo Scientific (35% solution); (v) Brazilian normal sand [14], with 96% silica content, using three granulometries, medium coarse (1.2–0.6 mm), medium fine (0.6–0.3 mm), and fine (0.3–0.15 mm), for the preparation of mortars.

The pastes were prepared using the following molar ratios: SiO_2/Al_2O_3 = 3.17, Na_2O/Al_2O_3 = 0.34, and SiO_2/Na_2O = 9.4. The mass composition used was 44% metakaolin, 52% sodium silicate solution, and 4% sodium hydroxide. H_2O_2 levels varying between 0 and 1% by mass of binder were used (Table 1). In the mortars, the composition was fixed at 1:2 (cement: sand), and the H_2O_2 content also ranged between 0 and 1% (Table 1).

Table 1. Concentration of hydrogen peroxide solution.

Paste	H_2O_2(%)	Mortar	H_2O_2(%)
P00	0	M00	0
P01	0.1		
P02	0.2	M02	0.2
P03	0.3		
P04	0.4	M04	0.4
P05	0.5		
P06	0.6	M06	0.6
P07	0.7		
P08	0.8	M08	0.8
P09	0.9		
P10	1.0	M10	1.0

The compositions were produced by a mechanical mixing process with the aid of a Contenco brand mixer involving the following steps: (i) homogenizing sodium silicate and sodium hydroxide at 60 rpm for 3 min; (ii) adding metakaolin at 60 rpm, for 3 min; (iii) adding H_2O_2 and mixing at 60 rpm for a further 2 min; and (iv) producing mortar by adding sand and mixing at 50 rpm for 3 min, before adding H_2O_2. The geopolymer was placed in cylindrical plastic molds (20 × 60 mm^2, for pastes, to be later cut in an Isomet 1000 cutting machine to the size of 20 × 40 mm^2) and prismatic metallic molds (40 × 40 × 160 mm^3, for mortars), which were then sealed with plastic film. The samples were cured under controlled conditions (24 °C and 70% relative humidity) for 24 h using a Hexasystems model HXCCu-40L climatic chamber. The samples were then demolded and kept sealed under the same curing conditions, for up to 28 days. A graphic summary showing the geopolymeric paste production process with the density and air content results can be seen in Figure 1.

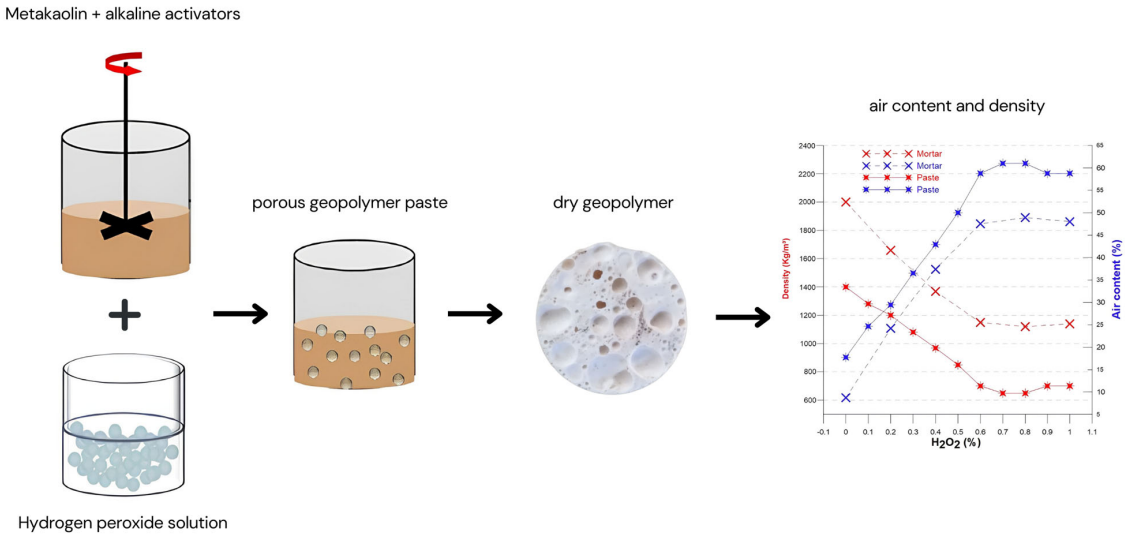


Figure 1. Graphic summary.

2.2. Material Characterization

The chemical composition of metakaolin was determined by X-ray fluorescence (Bruker D8 spectrometer) (Table 2). The particle size distribution was determined by laser diffraction (CILAS 1064 granulometer); the average diameter was 10.8 µm, the specific mass was 2510 kg/m^{3,} and the apparent density was 610 kg/m^3.

Table 2. Chemical composition of metakaolin.

Oxides	Wt. (%)
SiO_2	56.28
Al_2O_3	40.56
Fe_2O_3	0.66
K_2O	0.67
Other < 0.015	1.83
Loss on ignition (LOI)	1.75

2.3. Testing Methods and Equipment

The compressive strength was determined according to the ASTM 1231 [20]. The dynamic modulus of elasticity was determined according to ASTM E1876 [21] on Sonelastic equipment (ATCP physical engineering, laboratory NANOTEC, UFSC, Florianópolis, SC, Brazil).

Thermal conductivity at room temperature was determined using 20 × 10 mm^2 (diameter × height) tablets for pastes and 40 × 40 × 10 mm^3 prisms for mortars. A thermal properties analyzer (C-THERM TH130041, laboratory NANOTEC, UFSC, Brazil) using the modified transient plane source method according to ASTM D5334 [22] was used. Three samples per composition were used, and five readings were taken on each. The thermal conductivity in mortar plates (300 × 300 × 33 mm^3), based on the standard ASTM C-177 [23] and BS 874 [24], was also performed using a flow conductivity meter. The thermal test was performed in dry air conditions.

The thermal resistance was determined by the Fourier Law (Equation (1)):

$$R = \frac{T1 - T2}{\frac{q1-q2}{2}} \quad (1)$$

where R is the thermal resistance (m^2.K/W) of the material; q1 and q2 are the heat flow densities measured with flux meters 1 and 2 (W/m^2); and T1 and T2 are the surface sample temperatures determined by type T thermocouples, displayed in a differential arrangement.

Assuming a homogeneous sample, it is possible to determine the thermal conductivity of the material using the Equation (2), as follows:

$$\lambda = \frac{L}{R} \quad (2)$$

where λ is the thermal conductivity (W/m.K) and L is the sample thickness (m). The average temperature of the test was 25 °C.

The true density of the geopolymer prepared without H_2O_2, 1700 kg/m^3 (paste), and 2190 kg/m^3 (mortar) was determined by the pycnometry technique in helium gas, using the Archimedes principle of fluid displacement with the use of the Accu Pyc II 1340 equipment from micromeritics. The air content of GPs preparations, with the distinct addition of hydrogen peroxide, was then calculated according to the following equation by Landi et al. [25]:

$$\text{Air content}(\%) = \left[\left(1 - \left(\frac{\text{Apparent density}}{\text{True density}}\right)\right)\right] \times 100 \quad (3)$$

3. Results and Discussions

The effect of hydrogen peroxide (H_2O_2) in reducing the density of geopolymer pastes and mortars is shown in Figure 2. The density of the pastes steadily decreases as the foaming agent content in the compositions increases to 0.7 wt.%, before stabilizing at higher H_2O_2 contents. The composition containing 0.7 wt.% H_2O_2 (650 kg/m^3) shows a density roughly 50% lower than the non-foamed specimens (1400 kg/m^3). A similar trend was seen for the mortars, with a decrease from approximately 2000 kg/m^3 (reference) to 1200 kg/m^3 for a H_2O_2 concentration of 0.7 wt.%, a 40% reduction. The drop in the specimens' density is caused by the decomposition of H_2O_2, which releases oxygen gas and causes the material to expand, leading to the formation of voids [8,10]. The density of the reference mortar was typical of a conventional Portland cement mortar, ~2000 kg/m^3. The higher density of mortars compared to pastes (~35%) is attributed to the higher density of the aggregate (sand, 2600 kg/m^3) used in the composition and the initial air content, which might also reduce the expansion of the slurries.

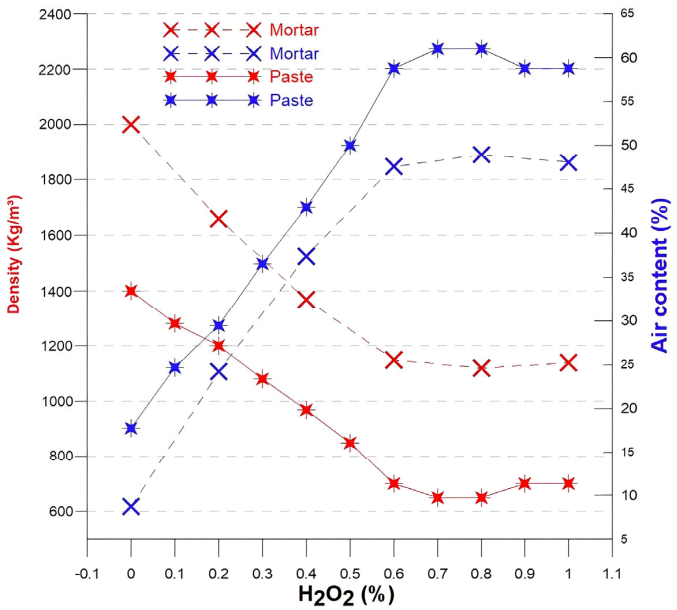
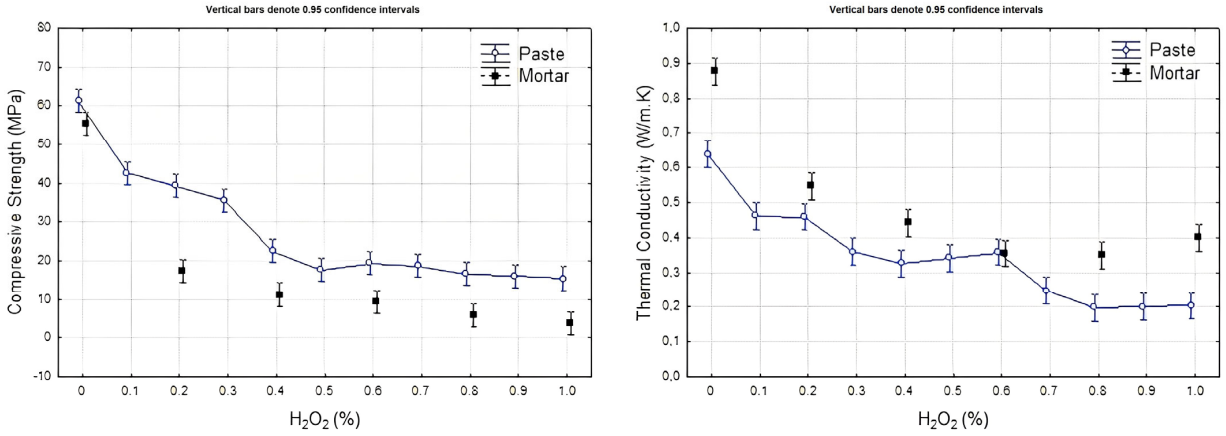


Figure 2. Effect of H_2O_2 on the apparent density of pastes and mortars.

An increase in the content of incorporated air (Figure 2) was also observed, up to a H_2O_2 concentration of 0.6%, which remained constant thereafter. These results stabilized

with approximately 50% porosity in the mortars and approximately 60% in the pastes. For lower H_2O_2 concentrations (0.1–0.4%), the effect on porosity was more significant.

The results for density and incorporated air are related to the results for compressive strength and thermal conductivity (Figure 3), in which a reduction in compressive strength was observed together with a reduction in thermal conductivity, up to a H_2O_2 concentration of 0.7%. The approximate reduction in compressive strength was 62 MPa to 18 MPa (at 0.7% H_2O_2), a reduction of 70%. Even with a significant reduction in strength, geopolymer compositions show high strength values, thus enabling their application in the production of building components. This feature is better perceived when comparing the values here reported with other literature studies dealing with the same topic (production of porous geopolymers); for this, we demonstrate, in Figure 4, the resistance to compression and the apparent density observed for several light geopolymers. As can be observed, the compressive strength of our specimen having a density of 550 kg/m^3 (16.6 MPa) is much higher those reported in (5.21 MPa; 550 kg/m^3) [26], (3 MPa; 585 kg/m^3) [6], (3.4 MPa; 640 kg/m^3) [6], (1.23 MPa; 560 kg/m^3) [27], and (0.78 MPa; 665 kg/m^3) [28], for specimens with comparable density.



(**a**) (**b**)

Figure 3. Effect of H_2O_2 concentration on the compressive strength (**a**) and thermal conductivity (**b**) of geopolymers pastes and mortars.

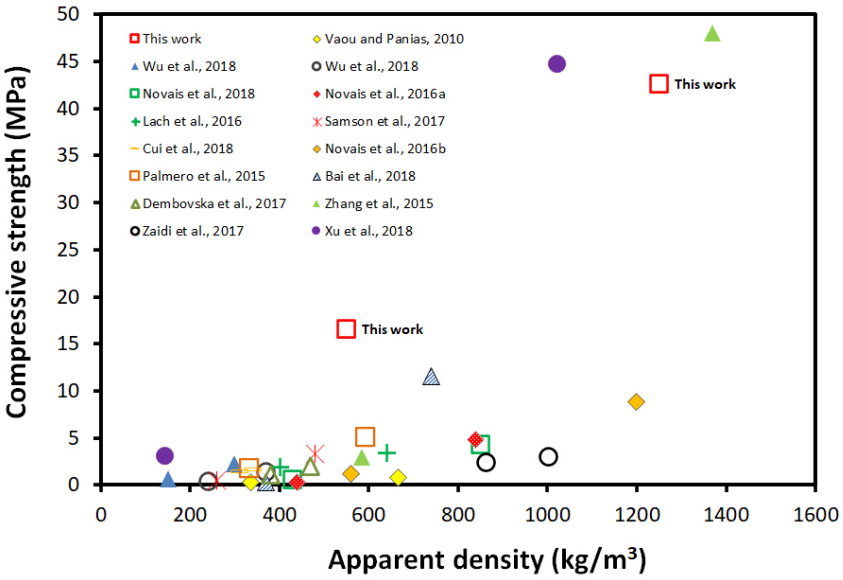


Figure 4. Review and literature comparison concerning compressive strength versus apparent density in lightweight geopolymer [8,11,12,14,15,26,28–34].

To better illustrate the merits of the present study, the specific strength (the ratio between the specimens' compressive strength and density) was determined and compared with other relevant literature studies, and the results are provided in Figure 5. The specific strength of the pastes synthesized in the present study ranged between 30.2 and 34.1 MPa cm^3/g, vastly superior to the majority of existing studies Palmero et al. [26], comparable to the maximum value reported by Zhang et al. [11] (35 MPa cm^3/g), and inferior to the maximum value seen in Xu et al. [15] (43.9 MPa cm^3/g). Nevertheless, the thermal conductivity reported in the latter study is higher (0.65 W/m.K) than the value observed in the present study (0.46 W/m.K).

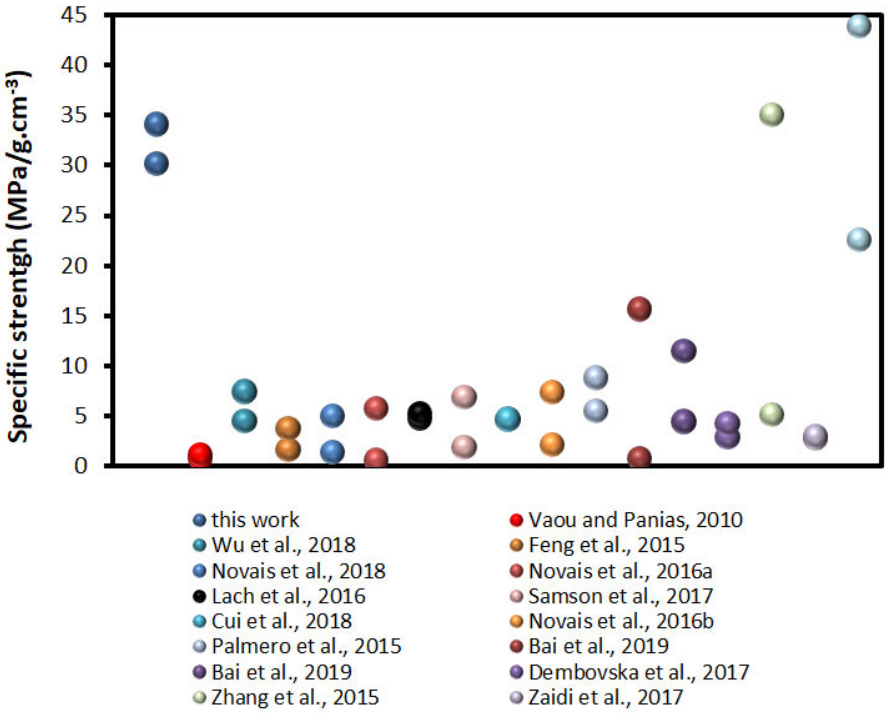


Figure 5. Review and literature comparison considering specific strength in lightweight geopolymer [8,11,12,26–35].

Thermal conductivity showed the same trend (Figure 3b), with a reduction from 0.58 W/(m.K) to 0.23 W/(m.K) (at 0.7% H_2O_2) of ~60%. Considering the results as a whole, a H_2O_2 concentration of 0.4% achieved a satisfactory compressive strength of ~34 MPa, thus ensuring its viability for use in the design and production of cladding panels in facades while also achieving a reduction in thermal conductivity of ~50%, down to 0.27 W/(m.K).

Regarding the mortar results, a greater reduction in strength was observed in mortars than in pastes (Figure 3a). In mortars, the concentration of H_2O_2 was altered in increments of 0.2% and, as observed for the pastes, stability was achieved for H_2O_2 concentrations above 0.6%. However, compressive strength values dropped from 55 MPa to ~10 MPa (at 0.6%), a reduction of approximately 80%. For thermal conductivity, the values dropped from 0.88 W/(m.K) to 0.36 W/(m.K), a reduction of ~60%, and presented very similar behavior to that observed in pastes. Considering the mechanical strength of mortar, a H_2O_2 concentration of 0.2% is the most suitable for its application since this achieves a compressive strength of ~18 MPa and an approximate thermal conductivity of 0.55 W/(m.K), 60% lower than the thermal conductivity measured in the reference composition. These results are competitive and efficient when compared with lightweight concrete and materials for greater thermal insulation.

The modulus of elasticity results in pastes and mortars (Figure 6) that follow a similar trend and relation to the results obtained in compressive strength, such that the results for pastes and mortars are very close though slightly higher in the pastes.

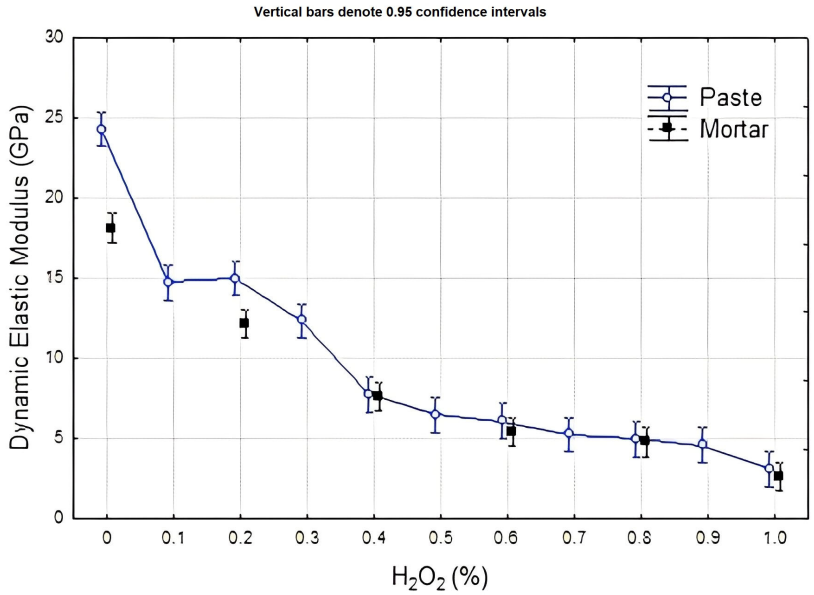


Figure 6. Effect of H_2O_2 concentration on the dynamic elastic modulus of the geopolymer.

In addition, thermal conductivity was measured in mortar panels (30 × 30 × 3 cm^3), using a heat flow meter (ASTM C-177, laboratory LMPT, UFSC, Brazil) [23], for the following compositions: reference 0%, 0.5%, and 1.0% H_2O_2 (Figure 7). The results obtained were 1.05 W/(m.K), 0.36 W/(m.K), and 0.40 W/(m.K) for H_2O_2 concentrations of 0%, 0.5%, and 1.0%, respectively. The thermal conductivity results were very close to those determined with the equipment C-THERM TH130041 (ASTM D-5334, laboratory NANOTEC, UFSC, Brazil) [22] used on the other samples. Thus, the geopolymer mortar (0.5% H_2O_2) showed a significant reduction in the thermal conductivity coefficient.



(**a**) (**b**)

Figure 7. Geopolymer mortar panels used in the thermal conductivity test 30 × 30 × 3 cm^3 (**a**), and image of geopolymer mortar with 0.8% H_2O_2 made with binocular stereomicroscope (**b**).

Regarding the findings as a whole, the simulation of the results of thermal transmittance on a facade was adopted as a criterion, and the mean thermal conductivity obtained for both types of panel was approximately 1.0 W/(m.K) (ref. geopolymer mortar) and 0.40 W/(m.K) (at 0.5% H_2O_2). Considering mortar panels, a total thermal resistance index

of 0.42 m^2.K/W and a thermal transmittance limit of 2.38 W/m^2.K can be achieved in a 10-cm-thick facade with a bioclimatic zone 3 classification [13]. This value is lower than the recommended thermal transmittance index (thermal transmittance $\leq$ 3.7 W/m) and the value for the reference geopolymer mortar (Table 3). This characteristic of improved thermal isolation contributes to building-energy efficiency and reduced operating costs in higher temperature environments.

Table 3. Thermal conductivity and thermal transmittance used for the mortars.

Material	Geopolymer Mortar	Lightweight Geopolymer Mortar (0.5% H_2O_2)
Thermal conductivity (W/m.K)	1.0	0.4
Thickness (cm)	10	10
Thermal resistance of mortar (m^2 K/W)	0.10	0.25
External surface thermal resistance (m^2 K/W)	0.04	0.04
Internal surface thermal resistance (m^2 K/W)	0.13	0.13
Total thermal resistance (m^2 K/W)	0.27	0.42
Thermal transmittance (W/m^2.K)	3.70	2.38
Limit—NBR 15.575 (W/m^2.K)	3.70	3.70

These results were not intended to determine an estimate of the heat load on a building or measure the overall operating costs involved but rather to show that the addition of H_2O_2 to the geopolymer mortar significantly improves the insulating capacity of the material, which reduces the thermal transmittance index and indicates its potential to improve thermal efficiency in buildings.

Measures aimed at saving energy in buildings and reducing greenhouse gas emissions are becoming increasingly important. Among these measures, the application of cold and reflective materials as building components has shown broad improvements in efficiency [36]. In addition to energy savings, the potential of reflective materials to reduce heat gains and improve thermal comfort in buildings has been confirmed by several studies [36]. Given this aim, whitish-colored metakaolin-based geopolymers (Figure 7) can potentially be classified as cold surfaces because they have low thermal conductivity; thus, they could contribute to thermal efficiency in buildings and the reduction in heat islands in large urban centers, leading to increased comfort and reduced energy costs while also contributing to the sustainability of the built environment.

4. Conclusions

In this study, the effect of the concentration of hydrogen peroxide on the production of light geopolymer pastes and mortars was evaluated, with the aim that these could be used as cladding panels on building facades. Thus, the thermal and mechanical properties were determined and showed that for pastes, a H_2O_2 concentration of 0.4% achieved a high compressive strength of 34 MPa with a reduction in thermal conductivity of ~50%, achieving a conductivity of 0.27 W/(m.K). Regarding mortars, a H_2O_2 concentration of 0.2% achieved a satisfactory mechanical strength of 18 MPa and thermal conductivity of 0.55 W/(m.K), 60% less than the thermal conductivity measured in the reference composition. The effect of H_2O_2 on the thermal conductivity and strength properties was significant up to a concentration of approximately 0.6%; above this concentration, it presented constant behavior, with no increase in pore formation.

Regarding mortar panels, a total thermal resistance index of 0.42 m^2K/W and a thermal transmittance limit of 2.38 W/m^2.K can be achieved in a 10-cm-thick facade with a bioclimatic zone 3 classification [13]. This value is lower than the recommended thermal transmittance index (thermal transmittance $\leq$ 3.7 W/m^2.K) and the value for the reference geopolymer mortar (3.7 W/m^2.K).

These results indicate the potential of geopolymer cements for use in the manufacture of construction materials, demonstrating their differentiated properties and their efficiency as materials for improving thermal comfort.

Author Contributions: Conceptualization, C.A. and F.P.; methodology, C.A.; software, C.A. and F.P.; validation, F.P., J.L. and R.N.; formal analysis, F.P.; investigation, C.A.; resources, F.P.; data curation, C.A.; writing—original draft preparation, C.A.; writing—review and editing, F.P., J.L. and R.N.; visualization, C.A.; supervision, F.P.; project administration, C.A.; funding acquisition, F.P., J.L. and R.N.; All authors have read and agreed to the published version of the manuscript.

Funding: This work was financially supported by the National Council for Scientific and Technological Development (CNPq, under number 304589/2019-5) and was developed within the scope of the CICECO-Aveiro Instituto de Materials project, UIDB/50011/2020, UIDP/50011/2020, and LA/P/0006/2020, funded by national funds through FCT/MEC (PIDDAC).

Data Availability Statement: Data is not available due to privacy.

Acknowledgments: This work had main financial support from the National Council for Scientific and Technological Development (CNPQ), we would like to thank the University of Aveiro, and the Institute of Materials (CICECO) for their contribution to this work, we would also like to thank Saulo Güths from LMPT/UFSC for providing us with thermal analysis data, and to Philippe Jean Paul Gleize from the laboratory NANOTEC/UFSC for providing us with equipment to carry out the tests.

Conflicts of Interest: The authors declare no conflict of interest.

References

1. Provis, J.L.; Palomo, A.; Shi, C. Advances in understanding alkali-activated materials. *Cem. Concr. Res.* **2015**, *78*, 110–125. [CrossRef]
2. McLellan, B.C.; Williams, R.P.; Lay, J.; van Riessen, A.; Corder, G.D. Costs and carbon emissions for geopolymer pastes in comparison to ordinary portland cement. *J. Clean. Prod.* **2011**, *19*, 1080–1090. [CrossRef]
3. Davidovits, J. Geopolymers. *J. Therm. Anal. Calorim.* **1991**, *37*, 1633–1656. [CrossRef]
4. Van Deventer, J.S.; Provis, J.; Duxson, P. Technical and commercial progress in the adoption of geopolymer cement. *Miner. Eng.* **2012**, *29*, 89–104. [CrossRef]
5. Novais, R.M.; Pullar, R.; Labrincha, J.A. Geopolymer foams: An overview of recent advancements. *Prog. Mater. Sci.* **2019**, *109*, 100621. [CrossRef]
6. Murri, A.N.; Medri, V.; Papa, E.; Laghi, L.; Mingazzini, C.; Landi, E. Porous Geopolymer Insulating Core from a Metakaolin/Biomass Ash Composite. *Environments* **2017**, *4*, 86. [CrossRef]
7. Lian, C.; Zhuge, Y.; Beecham, S. The relationship between porosity and strength for porous concrete. *Constr. Build. Mater.* **2011**, *25*, 4294–4298. [CrossRef]
8. Bai, C.; Colombo, P. Processing, properties and applications of highly porous geopolymers: A review. *Ceram. Int.* **2018**, *44*, 16103–16118. [CrossRef]
9. Jaya, N.A.; Yun-Ming, L.; Cheng-Yong, H.; Abdullah, M.M.A.B.; Hussin, K. Correlation between pore structure, compressive strength and thermal conductivity of porous metakaolin geopolymer. *Constr. Build. Mater.* **2020**, *247*, 118641. [CrossRef]
10. Gao, H.; Liao, L.; Liu, H.; Mei, L.; Wang, Z.; Huang, D.; Lv, G.; Zhu, G.; Wang, C. Optimization of thermal insulation performance of porous geopolymers under the guidance of thermal conductivity calculation. *Ceram. Int.* **2020**, *46*, 16537–16547. [CrossRef]
11. Zhang, Z.; Provis, J.L.; Reid, A.; Wang, H. Mechanical, thermal insulation, thermal resistance and acoustic absorption properties of geopolymer foam concrete. *Cem. Concr. Compos.* **2015**, *62*, 97–105. [CrossRef]
12. Łach, M.; Korniejenko, K.; Mikuła, J. Thermal Insulation and Thermally Resistant Materials Made of Geopolymer Foams. *Procedia Eng.* **2016**, *151*, 410–416. [CrossRef]
13. ABNT NBR 15498 NBR15498. Chapas Cimentícias Reforçadas Com Fios. Available online: https://www.target.com.br/produtos/normas-tecnicas/40441/nbr15498-chapas-cimenticias-reforcadas-com-fios-fibras-filamentos-ou-telas-requisitos-e-metodos-de-ensaio (accessed on 9 November 2021).
14. Novais, R.M.; Buruberri, L.; Ascensão, G.; Seabra, M.; Labrincha, J. Porous biomass fly ash-based geopolymers with tailored thermal conductivity. *J. Clean. Prod.* **2016**, *119*, 99–107. [CrossRef]
15. Xu, F.; Gu, G.; Zhang, W.; Wang, H.; Huang, X.; Zhu, J. Pore structure analysis and properties evaluations of fly ash-based geopolymer foams by chemical foaming method. *Ceram. Int.* **2018**, *44*, 19989–19997. [CrossRef]
16. Longo, F.; Lassandro, P.; Moshiri, A.; Phatak, T.; Aiello, M.A.; Krakowiak, K.J. Lightweight geopolymer-based mortars for the structural and energy retrofit of buildings. *Energy Build.* **2020**, *225*, 110352. [CrossRef]
17. Qadir, G.; Rashid, Y.; Hassan, A.; Vall, E.; Saleh, S.; Salim, K. Development and Mechanical Testing of Porous-Lightweight Geopolymer Mortar. *Buildings* **2020**, *11*, 1. [CrossRef]

18. Li, F.; Liu, L.; Yang, Z.; Li, S. Physical and mechanical properties and micro characteristics of fly ash-based geopolymer paste incorporated with waste Granulated Blast Furnace Slag (GBFS) and functionalized Multi-Walled Carbon Nanotubes (MWCNTs). *J. Hazard. Mater.* **2020**, *401*, 123339. [CrossRef]
19. Rashad, A.M. Metakaolin as cementitious material: History, scours, production and composition—A comprehensive overview. *Constr. Build. Mater.* **2013**, *41*, 303–318. [CrossRef]
20. *ASTM C1231/C1231M*; Standard Practice for Use of Unbonded Caps in Determination of Compressive Strength of Hardened Cylindrical Concrete Specimens. ASTM International: West Conshohocken, PA, USA, 2015. Available online: https://www.astm.org/Standards/C1231 (accessed on 16 February 2023).
21. *ASTM E 1876:01*; Standard Test Method for Dynamic Young's Modulus, Shear Modulus, and Poisson's Ratio by Impulse Excitation of Vibration. Book of Standards, vol. i, no. C. pp. 1–15. 2009. Available online: https://www.astm.org/Standards/E1876.htm (accessed on 16 February 2023).
22. *ASTM D5334*; Standard Test Method for Determination of Thermal Conductivity of Soil and Soft Rock by Thermal Needle Probe Procedure. Available online: https://www.astm.org/Standards/D5334.htm (accessed on 16 February 2023).
23. U. States. Standard Test Method for Steady-State Heat Flux Measurements and Thermal Transmission Properties by Means of the Guarded-Hot-Plate, Annual Book of ASTM Standards, No. C. 2009. Available online: https://www.astm.org/Standards/C177.htm (accessed on 16 February 2023).
24. *BS 874*; Methods for Determining Thermal Insulating Properties with Definitions of Thermal Insulating Terms. Available online: https://global.ihs.com/doc_detail.cfm?document_name=BS%20874&item_s_key=00139968 (accessed on 16 February 2023).
25. Landi, E.; Medri, V.; Papa, E.; Dedecek, J.; Klein, P.; Benito, P.; Vaccari, A. Alkali-bonded ceramics with hierarchical tailored porosity. *Appl. Clay Sci.* **2013**, *73*, 56–64. [CrossRef]
26. Palmero, P.; Formia, A.; Antonaci, P.; Brini, S.; Tulliani, J.-M. Geopolymer technology for application-oriented dense and lightened materials. Elaboration and characterization. *Ceram. Int.* **2015**, *41*, 12967–12979. [CrossRef]
27. Novais, R.M.; Ascensão, G.; Buruberri, L.; Senff, L.; Labrincha, J. Influence of blowing agent on the fresh- and hardened-state properties of lightweight geopolymers. *Mater. Des.* **2016**, *108*, 551–559. [CrossRef]
28. Vaou, V.; Panias, D. Thermal insulating foamy geopolymers from perlite. *Miner. Eng.* **2010**, *23*, 1146–1151. [CrossRef]
29. Wu, J.; Zhang, Z.; Zhang, Y.; Li, D. Preparation and Characterization of Ultra-Lightweight Foamed Geopolymer (UFG) *Based on Fly Ash-Metakaolin Blends*. *Constr Build Mater* **2018**, *168*, 771–779. [CrossRef]
30. Novais, R.M.; Gameiro, T.; Carvalheiras, J.; Seabra, M.P.; Tarelho, L.A.C.; Labrincha, J.A.; Capela, I. High PH Buffer Capacity Biomass Fly Ash-Based Geopolymer Spheres to Boost Methane Yield in Anaerobic Digestion. *J. Clean. Prod.* **2018**, *178*, 258–267. [CrossRef]
31. Cui, Y.; Wang, D.; Zhao, J.; Li, D.; Ng, S.; Rui, Y. Effect of Calcium Stearate Based Foam Stabilizer on Pore Characteristics and Thermal Conductivity of Geopolymer Foam Material. *J. Build. Eng.* **2018**, *20*, 21–29. [CrossRef]
32. Dembovska, L.; Bajare, D.; Ducman, V.; Korat, L.; Bumanis, G. The Use of Different By-Products in the Production of Lightweight Alkali Activated Building Materials. *Constr. Build Mater.* **2017**, *135*, 315–322. [CrossRef]
33. Zaidi, S.F.A.; Ul Haq, E.; Nur, K.; Ejaz, N.; Anis-ur-Rehman, M.; Zubair, M.; Naveed, M. Synthesis & Characterization of Natural Soil Based Inorganic Polymer Foam for Thermal Insulations. *Constr. Build Mater.* **2017**, *157*, 994–1000. [CrossRef]
34. Samson, G.; Cyr, M.; Gao, X.X. Thermomechanical Performance of Blended Metakaolin-GGBS Alkali-Activated Foam Concrete. *Constr. Build Mater.* **2017**, *157*, 982–993. [CrossRef]
35. Feng, J.; Zhang, R.; Gong, L.; Li, Y.; Cao, W.; Cheng, X. Development of Porous Fly Ash-Based Geopolymer with Low Thermal Conductivity. *Mater. Des.* **2015**, *65*, 529–533. [CrossRef]
36. Hernandez-Perez, I.; Alvarez, G.; Xaman, J.; Zavala-Guillen, I.; Arce, J.; Sima, E. Thermal Performance of Reflective Materials Applied to Exterior Buildings Components-A Review. *Energy Build.* **2014**, *80*, 81–105. [CrossRef]

Disclaimer/Publisher's Note: The statements, opinions and data contained in all publications are solely those of the individual author(s) and contributor(s) and not of MDPI and/or the editor(s). MDPI and/or the editor(s) disclaim responsibility for any injury to people or property resulting from any ideas, methods, instructions or products referred to in the content.